Memoirs of the Faculty of Engineering, Kyushu University, Vol. 71, No. 4, December 2011

Validation of Trampoline Effect for Earthquake Induced Landslides using Numerical Analysis

by

Lu ZHENG[*], Guangqi CHEN[**], Kouki ZEN[***]
and Kiyonobu KASAMA[**]

(Received October 20, 2011)

Abstract

Trampoline effect is introduced to interpret the mechanism of long run-out movement of earthquake-induced landslide in Multiplex Acceleration Model (MAM). In previous study, this model was verified by a shaking table test. However, there is a scale limitation of shaking table test to investigate MAM in detail. Thus, numerical simulation was carried out in this study to validate MAM with respect to field phenomenon in Wenchuan Earthquake (Ms. 8.0). A truck threw upwards by seismic force was discussed based on the simulation results. The results indicate that trampoline effect could be composed by continuous collisions in P-Phases of earthquake and makes the intensity grow up. The results show that MAM is acceptable and applicable.

Keywords: Earthquake-induced landslides, Long runout, Multiplex Acceleration Model, Trampoline effect, UDEC

1. Introduction

During the last 15 years, after a series of catastrophic earthquake events in Japan (1995), Taiwan (1999), El Salvador (2001), Pakistan (2005) and China (2008), increasing attention has been addressed to landslides triggered by earthquakes.

Due to the strong ground motion of earthquake, the landslide can travel a distance several times longer than the height of the slope at a high velocity and result in great damages and losses[1, 2, 3, 4, 5, 6]. For example, there were many landslides with run-out distances over 1000m triggered by the 2008 Wenchuan Earthquake (Ms. 8.0). **Figure 1** shows a typical long run-out landslide induced in Donghekou, Qingchuan prefecture of Sichuan province, China. It traveled around 2800m within 80s.

[*] Ph.D. Candidate, Department of Civil and Structural Engineering
[**] Associate Professor, Department of Civil and Structural Engineering
[***] Professor, Department of Civil and Structural Engineering

(a) Before earthquake (b) After earthquake

Fig. 1 The landslide induced by the 2008 Wenchuan Earthquake in Donghekou, Qingchuan prefecture of Sichuan Province, China.

However, in Japan, the "Law concerning disaster prevention due to landslide" has been promulgated and adopted by the government since 2003[7]. The Dangerous Area for a potential landslide is identified as 2 times of slope height but less than 50m in this law (**Fig. 2**). It is established based on statistics of the run-out distances in historical events, which were mainly triggered by heavy-rains.

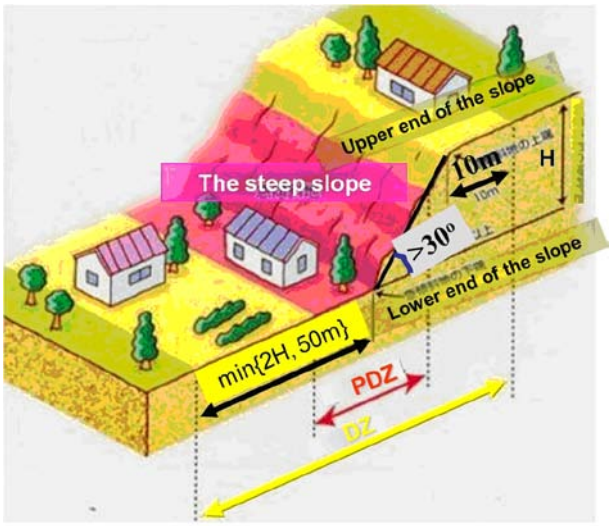

Fig. 2 Dangerous Zone defined by the "Law concerning disaster prevention due to landslide" in Japan.

It is obviously that the Dangerous Zone defined in the law is not enough for earthquake-induced landslides. Therefore, it is very important to investigate the mechanism of high speed & long distance and its runout zone to predict the Dangerous Zone.

Analyses performed according to the Newmark[8] approach at regional scale allow developing different earthquake triggered landslide scenarios[9, 10, 11, 12, 13]. These sliding block models are based on the simplifying assumption that the sliding mass is rigid. Among its deficiencies: it provides limited information on the evolution of the landslide and does not reproduce the mechanisms of deposition of the slope material. On the other hand, elasto-plastic continuum models[2, 14, 15] fully considered the deformability of the sliding mass are capable of simulating the formation and development of shear zones with realism, thereby leading to improved modeling failure mechanism.

And if assuming the sliding mass behaves as a liquid mixture of fluids and solids, depth-integrated models can be used in modeling post-liquefaction behavior of granular soil induced by earthquake[16].

According to field investigation, the landslides in Wenchuan Earthquake could be illustrated by following characteristic: the debris mass was separately expanded and thrown under long-period strong ground vibration[17]. It can be interpreted that debris mass consist of rock fragments is not a continuum, its behavior due to presence of joint sets, bedding planes and faults etc. Moreover, some landslide sites are relatively dry. Thus, the current mechanisms and models such as Liquefaction[18], flow mechanism[19, 20] which are mainly continuum, flow like and concentrating on the loss of material strength, are not adapt for these cases. Then in order to interpret the long run-out mechanism of landslide triggered by earthquake and predict its runout, a new model called "Multiplex Acceleration Model" (MAM) was proposed base on consideration of the "trampoline effect" during earthquake[7]. Subsequently, this model tests were verified by a shaking table test investigating the effects of earthquake on the movement of debris. However, it is difficult to distinguish the trampoline effect from ground motion of earthquake since the scale limitation.

In geotechnical practice, it is a commonly used discrete element approach for investigating the kinematics of landslides. Using detail geological and geotechnical data, DEM or DDA can be used to interpret the post-failure movement of landslide masses in good agreement with filed investigation[21, 22, 23]. In this study, we have attempted to simulate the phenomenon of velocity of debris gained from the vibration of the slope and its further amplification during an earthquake using the Universal Distinct Element Code (UDEC) developed by Cundall[24, 25, 26].

2. Multiplex Acceleration Model

2.1 Earthquake Behavior on Slope and Debris

The vibration of a slope caused by earthquake wave can be divided into two phases: P-phase and N-phase as shown in **Fig. 3**. The P-phase is defined as the period when the slope is moving in the outer normal direction of the slope surface. The debris on the surface will be pushed and accelerated by the slope in this phase. The N-phase is defined as the period when the slope is moving in the inner normal direction of the slope surface. Since slope surface moves apart from the debris, the friction should be declined.

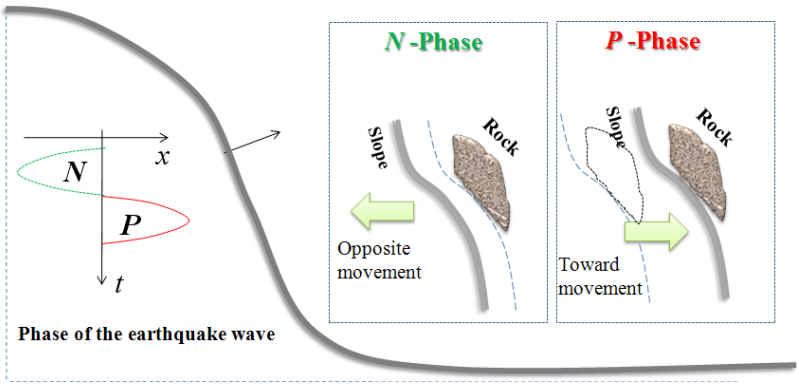

Fig. 3 Definitions of P-Phases and N-Phases.

2.2 Energy Analysis

The roles of the two phases can be seen more clearly by apparent friction angle analysis when considering energy conservation. Supposing that a stone with mass *m* moves from position A to

position B_1 during a landslide without earthquake (Case 1), the potential energy decreases by *mgh*. Based on the energy conservation law, it is easy to obtain the following equation for a falling stone movement in the case without earthquake (see Case 2 in **Fig. 4**).

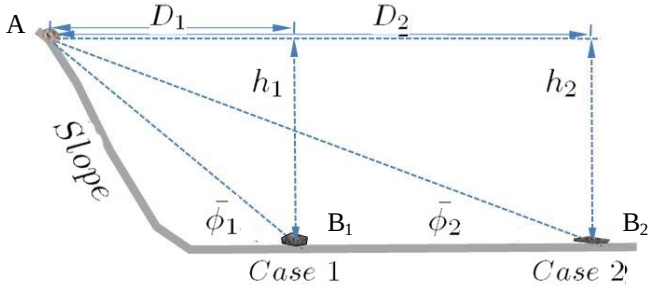

Fig. 4 Apparent friction angle.

$$mgh - \sum_i l_i mgk_i \tan\phi_{si} \cos\theta_i = 0 \tag{1}$$

The first term here is for potential energy and the second item is for the work of friction force between the slope and the falling stone, where the sliding movement is considered and the whole curve path is divided into finite linear segments. And *m* is the mass, *g* is the gravity acceleration, *h* is the falling height, *l* is the segment length, θ is the segment slope angle, ϕ is the friction angle, *k* is the coefficient of conveying from static to dynamic friction and *i* is the index of segment.
The apparent friction angle can be obtained from Eq. (1) as follows:

$$\tan\bar{\phi}_1 = \frac{h_1}{D_1} = \sum_i w_i k_i \tan\phi_{si} \tag{2}$$

The apparent friction angle expressed in Eq. (2) is usually used for the discussion of run-out distance of landslide.

When we consider the effects of slope vibration due to earthquake (mass moves to B_2), the kinetic energy of falling stone obtained from the collision with the vibrating slope and the movement patterns (sliding, rolling and flying) should be considered. Thus, Eq. (1) becomes:

$$mgh + \sum_i \frac{1}{2} m v_{ej}^2 - \sum_i l_i mgk_i^* \tan\phi_{si} \cos\theta_i = 0 \tag{3}$$

The second item here is for the kinetic energy of a falling stone obtained from the collision with the vibrating slope and v_{ej} is the velocity obtained in j^{th} P-phase and can be expressed as follows:

$$v_{ej} = VTR \int_{t_i}^{t_i+\Delta t} f(t)dt \tag{4}$$

is the acceleration of slope vibration due to earthquake, *VTR* is called the velocity transmission ratio due to collision.

The apparent friction angle for the Case 2 in **Fig. 4** can be obtained from Eq. (3) as follows:

$$\tan\bar{\phi}_2 = \frac{h_2}{D_2} = \sum_i w_i k_i^* \tan\phi_{si} - \frac{1}{2gD_2} \sum_j v_{ej}^2 \tag{5}$$

Comparing Eq. (5) with Eq. (2), it can be found that:

(1) The kinetic energy of a falling stone obtained from the collision with the vibrating slope may result in long run-out distance from the second item of Eq. (5).
(2) The coefficient of conveying from static to dynamic friction k^* in Eq. (5) can be smaller than *k*

in Eq. (3) because of the N-Phase effect, air cushion effect, movement pattern.

Detail discussion will be given in the following sections.

Collision Effect

In P-phase, a falling stone can obtain kinetic energy from the colliding with the vibrating slope. According to elastic collision theory, when two objects with different masses collide with each other, the object with smaller mass could obtain larger velocity. Since the mass of a slope is much larger than the mass of a falling stone, the velocity of the falling stone can be much larger than the vibrating velocity of the slope. That is to say the *VTR* in Eq. (6) can be larger than 1.

$$VTR = \frac{V_{21}}{V_{10}} \tag{6}$$

The *VTR* can be examined by the simple model shown in **Fig. 5**. The masses of the two blocks are m_1 and m_2 respectively. Before the colliding, the block 1 has initial velocity V_{10} toward block 2 which is standstill, $V_{20} = 0$. The friction between blocks and the base is negligible. After the colliding, the velocity of block 1 becomes V_{11} while block 2 obtains a velocity V_{21}.

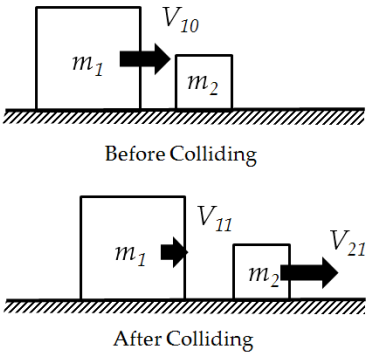

Fig. 5 Colliding model.

According to the principles of the conservation of both energy and momentum:

$$\frac{1}{2}m_1V_{10}^2 + \frac{1}{2}m_2V_{20}^2 = \frac{1}{2}m_1V_{11}^2 + \frac{1}{2}m_2V_{21}^2 \tag{7}$$

$$m_1V_{10} + m_2V_{20} = m_1V_{11} + m_2V_{21} \tag{8}$$

By solving Eq. (7) and Eq. (8), the *VTR* for the case of $V_{20} = 0$ can be obtained as follows:

$$VTR = \frac{2m_1}{m_1 + m_2} \tag{9}$$

It can be seen from the analytical solution Eq. (9) that if m_1 is much larger than m_2, *VTR* is to approach to 2. Therefore, since the mass of a slope is far larger than the falling stone, the velocity of the falling stone obtained from the slope vibration will be two times of that of the slope vibration velocity during earthquake.

The results of *VTR* given in analytical solution Eq. (9) have been verified by UDEC simulation. The model shown in **Fig. 5** and the parameters given in **Table 1** are used in UDEC simulations. The results obtained from UDEC simulations by changing m_1 are shown in **Fig. 6**, together with the theoretical analytical values. The line is calculated from the analytical solution Eq. (9) and the circle dots are obtained from UDEC simulations. It can be seen that the *VTR* obtained from UDEC is in quite good agreement with the analytical solution.

Table 1 Parameters used in UDEC simulations.

Parameters	Value
Density (kg/m^3)	2000
Bulk Modulus (MPa)	2.78×10^3
Shear Modulus (MPa)	2.08×10^3
Contact Stiffness (KN/m)	1.00×10^6
Fraction of critical damping	0.005
Frequency (Hz)[a]	91.52

[a]Frequency is estimated by Young's modulus.

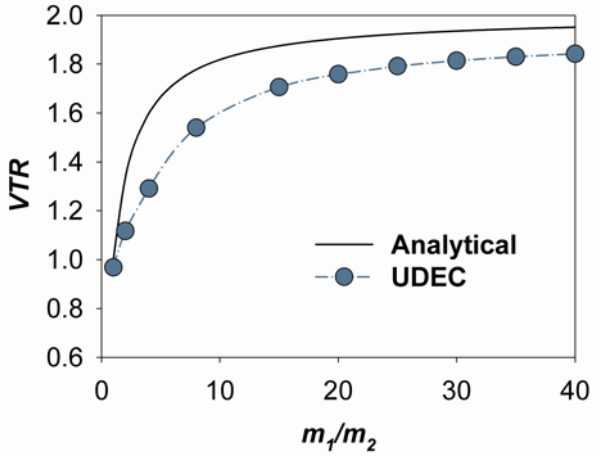

Fig. 6 *VTR* obtained by both the analytical solution and UDEC simulation.

Trampoline Effect

Furthermore, if the block 2 has an initial velocity toward block 1, the *VTR* could become larger and larger as shown in **Fig. 7**. It indicates trampoline effect can be produced by strong earthquake.

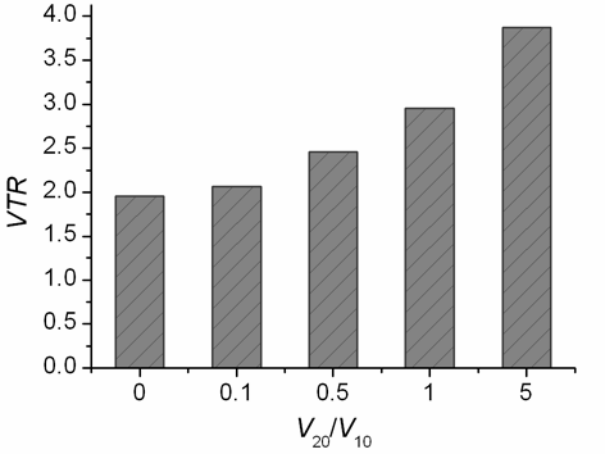

Fig. 7 Trampoline effect with V_{20} increasing.

It should be pointed out that the results do not change when the mass and the initial velocity of block one are different from the values in **Table 1**. That is to say, the result given in **Fig. 6** and **7** has the general meaning.

3. Verification with Respect to Field Phenomenon

In the 2008 Wenchuan Earthquake (Ms. 8.0), the records of acceleration showed that very large PGA. In some place, the vertical PGA was even bigger than horizontal PGA. **Figure 8** shows a truck was found leaning against the wall after earthquake. It indicated a strong vertical seismic wave caused this phenomenon.

Fig. 8 Truck threw up by vertical seismic wave (from Prof. Tang).

Figure 9 is a simple model used to simulate it. It is supposed that the truck was not beside the house at first. The phenomenon is induced by both vertical and horizontal wave. However, to a trampoline movement, the vertical wave is primary. To simplify the simulation, the horizontal wave is neglected and the truck is set next to the house instead.

The parameters are listed in **Table 2** and **3**. A joint with strong Cohesion, Tension value and large Friction angle was used to fix the house on the base land and wheels on truck. Considering this model was limited near the ground surface and neglecting the effect of wave propagation, the base ground was treated as vibrating like a whole one and the earthquake acceleration was added on all the mesh vertices after turning into velocity wave.

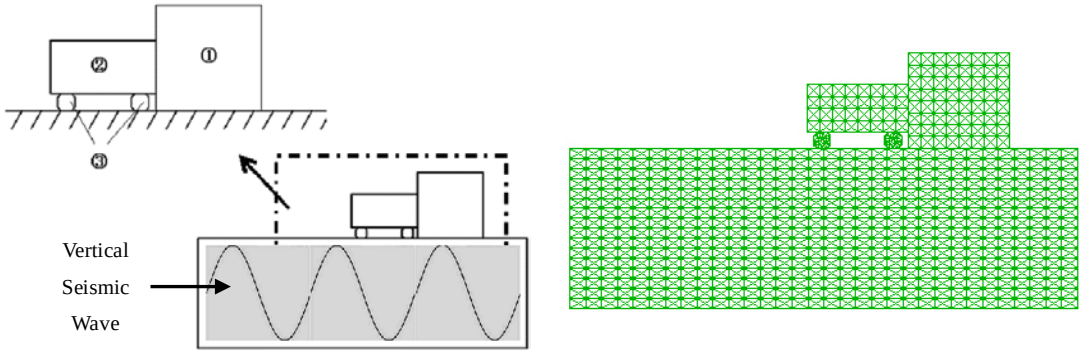

(a) Model scheme (b) Mesh generation in UDEC

Fig. 9 Simulation model of truck threw up.

Since: (1). There is no earthquake record station nearby the study area; (2). Earthquake wave is largely affected by geology, topography et al., the real earthquake curves in this area is not available and the recorded waves are not suitable to use. However, the PGA can be used to present the earthquake strength. So a simple harmonic wave as part of earthquake with the same PGA is

used to simulate the phenomenon in orders to qualitatively analysis the mechanism firstly. In this study, a sine wave of velocity, which is turned into stress wave, was used in the simulation as shown in **Fig. 10**. The left part is input velocity wave, and the right part is output acceleration wave at base of the ground in order to validate the input PGA. The wave presented PGA 1500 gal, Frequency 3.5Hz, according to that there was a PGA = 1500 gal recorded at a strong motion station in Zipingpu dam region.

Table 2 Physico-mechanical parameters.

Parameters	①	②	③
Density (kg/m^3)	2000	3000	2000
Bulk Modulus (MPa)	2.78×10^3	2.78×10^3	2.78×10^1
Shear Modulus (MPa)	2.08×10^3	2.08×10^3	2.08×10^1

①: Building and Base ground; ②: Truck body; ③: Wheel

Table 3 Mechanical parameters of joint.

Parameters	A	b
Kn (MPa/m)	5.0×10^3	5.0×10^3
Ks (MPa/m)	5.0×10^3	5.0×10^3
Tension (MPa)	0.0	1.0×10^3
Cohesion (MPa)	0.0	1.0×10^3
Friction Angle (°)	30.0	70.0

a: joints between wheels and base ground;

b: joints between wheels and truck, house and baseground;

The values of joint parameters Kn and Ks are chosen as high accuracy in colliding simulation[27].

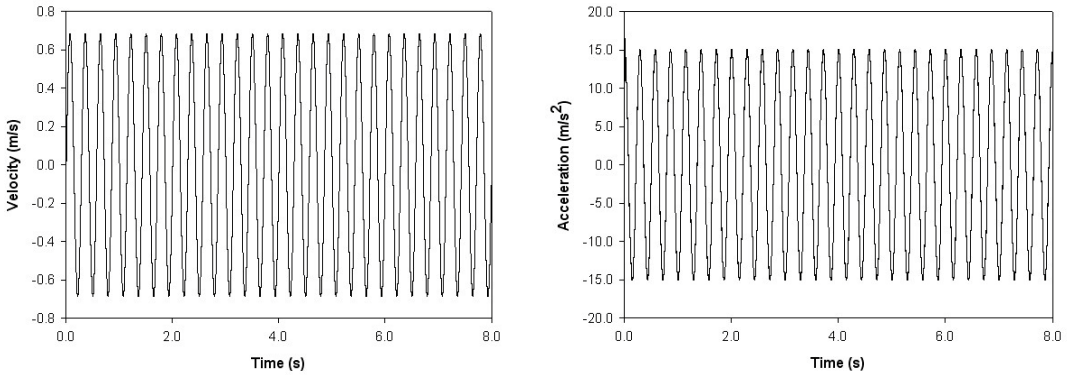

(a) Input velocity wave (b) Output acceleration wave for validation

Fig. 10 Input vertical seismic acceleration: PGA, 1500gal, frequency, 3.5Hz.

The movements of truck at different times obtained from UDEC simulation are shown in **Fig. 11**. The rotation displacement is very small at very beginning. But following results show that the truck was threw up higher and higher with time passing by the trampoline effect.

Figure 12 and **13** is the velocity and displacement results of simulation. Black line is the displacement and velocity at tail of truck. Blue lines are the positive part of base displacement. They show the P-Phases in which base moved upward to the truck; Red lines show the N-Phases in which base moved apart from the truck. The intersection points of two lines indicate the collisions. The green boundary lines show that the trampoline effect occurs. **Figure 14** clearly shows that

almost all the intersection points located at the blue part. That means collisions threw the truck up which almost happened at the P-Phases. It also indicates that if collisions in P-Phases continue, the collision effect would turn to a trampoline movement.

A series of earthquake waves were used to investigate this trampoline effect more detail as listed in **Table 4**.

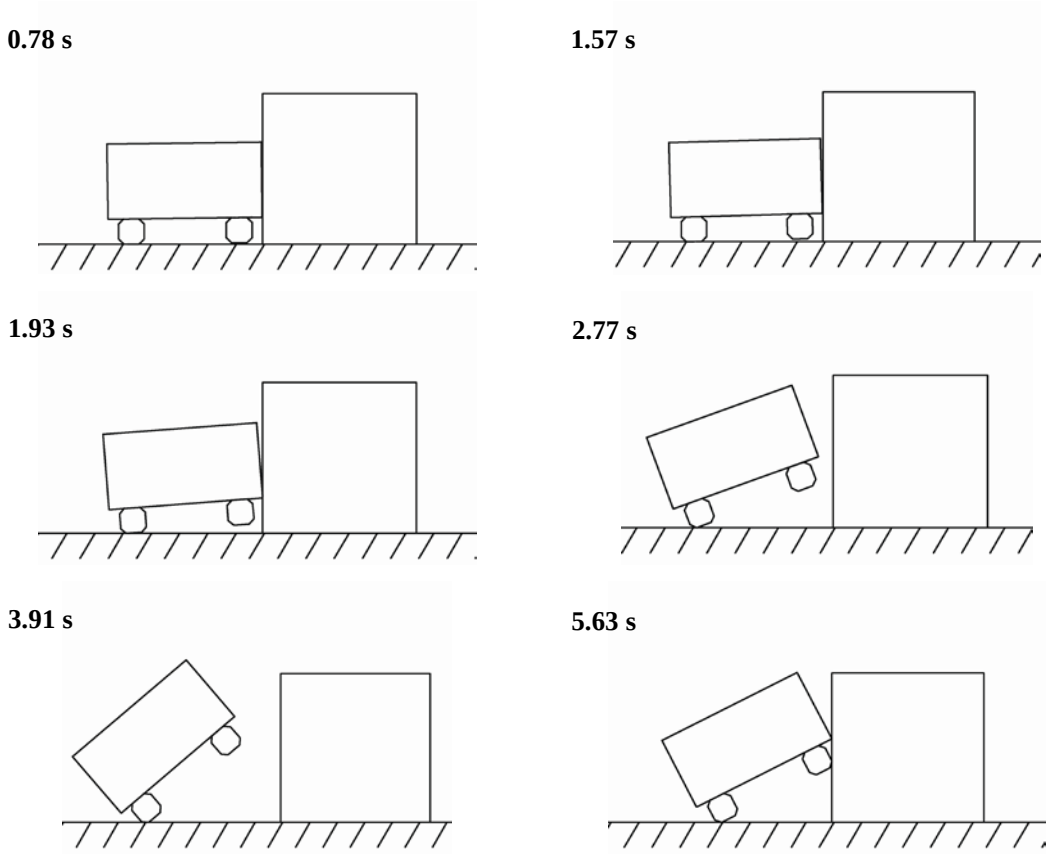

Fig. 11 Results of truck threw up in UDEC simulation: PGA, 1500gal, frequency, 3.5Hz.

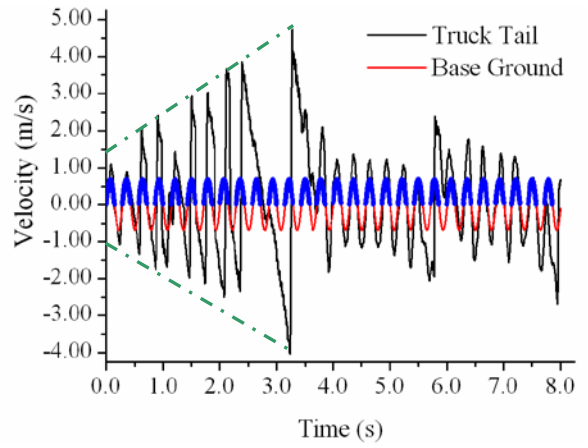

Fig. 12 Results of velocity vs time: PGA, 1500gal, frequency, 3.5Hz.

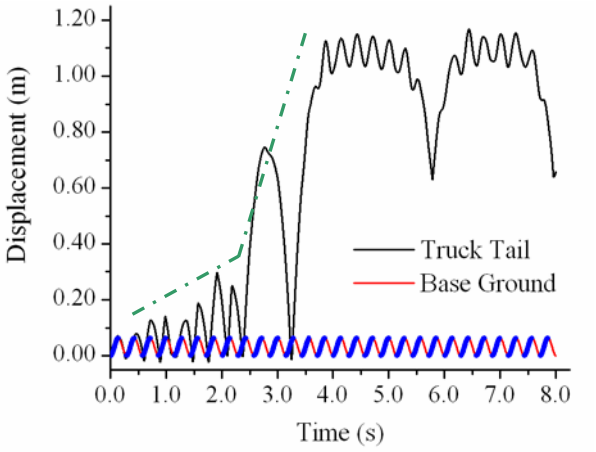

Fig. 13 Results of displacement vs time: PGA, 1500gal, frequency, 3.5Hz.

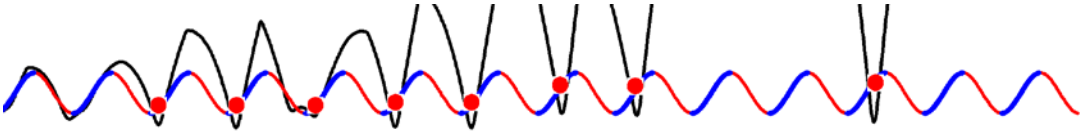

Fig. 14 Almost all collisions located in P-phases: red point means collision in P-Phases.

Table 4 Input vertical seismic wave case list.

Case.	Frequency (Hz)	PGA (gal)	Trampoline	Case.	Frequency (Hz)	PGA (gal)	Trampoline
1	2.0	1400	√	7	3.0	1500	X
2	2.5	1400	√	8	3.5	1500	√
3	3.0	1400	√	9	2.0	1600	√
4	3.5	1400	X	10	2.5	1600	√
5	2.0	1500	√	11	3.0	1600	X
6	2.5	1500	√	12	3.5	1600	√

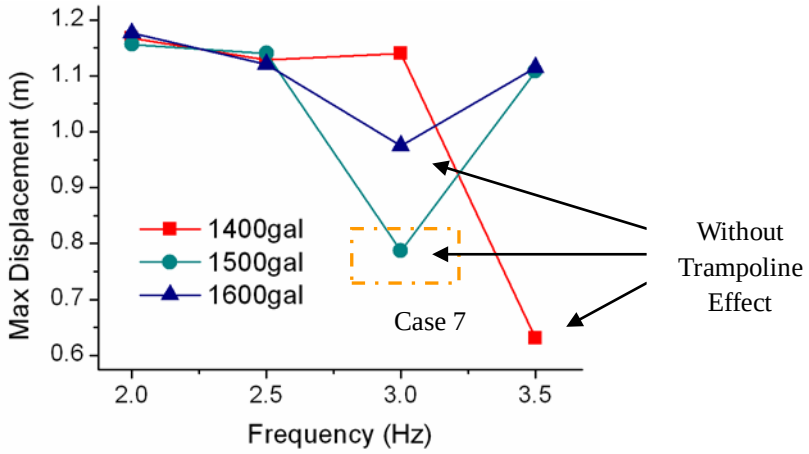

Fig. 15 Largest bounce heights.

The results of the largest bounce height are shown in **Fig. 15**. Although most cases reach the same maximum displacement since 1400gal, some cases the trampoline effect is not enough to produce a significant phenomenon, which are 1400gal, 3.5Hz, 1500gal, 3.0Hz and 1600gal 3.0Hz. Take case 7: 1500gal, 3.0Hz as example, the displacement result is shown in **Fig. 16**. As using the same setting as **Fig. 12**, black line is the displacement and velocity at tail of truck. Blue lines show the P-Phases of base movement and red lines show the N-Phases.

Figure 15 also shows that the displacements of trampoline effect are much larger than those without trampoline effect.

The detail collision situations in case 7 are shown in **Fig. 17**. The intersection points indicate the collisions. In which, the green ones are located in N-Phases and red ones are in P-Phases. It can be clearly found that, since many collisions did not occur in P-Phases, it cannot generate significant trampoline effect as shown in **Fig. 16**.

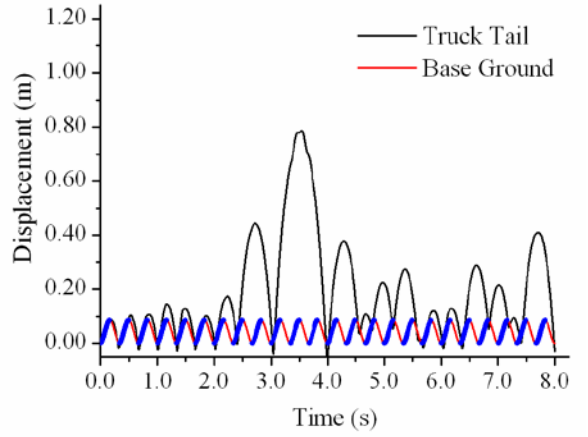

Fig. 16 Results of displacement vs time: PGA, 1500gal, frequency, 3.0Hz.

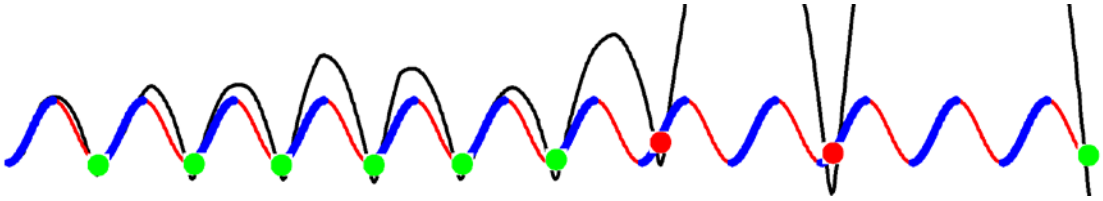

Fig. 17 Collisions in Case 7: green points mean collisions not in P-Phases.

4. Conclusion

According to the Multiplex Acceleration Model, the earthquake behaviours of a slope caused by earthquake wave can be divided into two phases: P-Phase and N-Phase. By energy analysis, the collision in P-Phases, further trampoline effect and move patterns change can produce the long runout.

The verification studies, presented here, illustrate the important behavior of Multiplex Acceleration Model to interpret the mechanism of high-speed and long run-out landslide with respect to both analytical solution and filed data. Specifically,

(1) Collision effects at P-phase can be an important factor which would cause high-speed and long run-out landslide;

(2) Further, it will turn to trampoline effect consist of continuous collisions in P-Phases which will

make the intensity grow up.

The results indicate it is acceptable and applicable to use Multiplex Acceleration Model to analysis earthquake induced landslide disasters by considering trampoline effect.

Acknowledgements

The presented research work and the preparation of this paper have received financial support from the Global Environment Research Found of Japan (S–4), Grants-in-Aid for Scientific Research (Scientific Research (B), 19310124, G. Chen) from JSPS (Japan Society for the Promotion of Science). These financial supports are gratefully acknowledged.
The editorial committee would like to hear comments, advices or questions (if any) on usage of this template, thus it may be always improved.

References

1) Keefer, D. K.; “Landslides caused by earthquakes”, Geol. Soc. Am. Bull., Vol.95, p. 406-421 (1984).
2) Sassa, K.; “Prediction of earthquake induced landslides”. Landslides. Balkema, Rotterdam, pp. 115-132 (1996).
3) Rodriguez, C. E., Bommer, J. J., Chandler, R. J.; “Earthquake-induced landslides: 1980–1997”, Soil. Dyn. Earthq. Eng., Vol.18, pp. 325-346 (1999).
4) Keefer, D. K.; “Investigating landslides caused by earthquakes - A historical review”, Surv. Geophys., Vol.23, No.6, pp. 473-510 (2002).
5) Bird, J. F., Bommer, J. J.; “Earthquake losses due to ground failure”, Eng. Geol., Vol.75, pp.147-179 (2004).
6) Havenith, H. and Bourdeau, C.; “Earthquake-induced landslide hazards in mountain regions: A review of case histories from central Asia”, Geol. Bel., Vol.13, No.3, pp. 137-152 (2010).
7) Chen, G. Q., Zen, K., Zheng, L. and Jiang, Z. S.; “A new model for long-distance movement of earthquake induced landslide”, Proceedings of the 44th U.S. Symposium on Rock Mechanics, Salt Lake City, UT, USA (2010).
8) Newmark, N. M.; “Effects of earthquakes on dams and embankments”, Geotechnique Vol.15, pp. 139-159 (1965).
9) Luzi, L., Pergalani, F.; “Application of statistical and GIS techniques to slope instability zonation (1:50,000 Fabriano geological map sheet)”, Soil. Dyn. Earthq. Eng., Vol.15, pp. 83-94 (1996).
10) Miles, S. B., Ho, C. L.; “Rigorous landslide hazard zonation using Newmark’s method and stochastic ground motion simulation”, Soil. Dyn. Earthq. Eng., Vol.18, No.4, pp. 305–323 (1999).
11) Romeo, R.; “Seismically induced landslide displacements: a predictive model”, Eng. Geol., Vol. 58 No.(3/4), pp. 337-351 (2000).
12) Chang, K. J., Taboada, A., Lin, M. L., Chen, R. F.; “Analysis of landsliding by earthquake shaking using a block on slope thermo-mechanical model: Example of Jiufengershan landslide, central Taiwan”. Eng. Geol., Vol.80, pp. 151-163 (2005).
13) Mahdavifar, M., Jafari, M. K., Zolfaghari, M. R.; “GIS-based real time prediction of Arias intensity and earthquake-induced landslide hazards in Alborz and Central Iran”, Landslides and engineered slopes. Taylor and Francis Group, London. ISBN: 978-0-415-41196-7, pp.1427-1438 (2008).

14) Vardoulakis, I.; "Dynamic thermo-poro-mechanical analysis of catastrophic landslides", Geotechnique, Vol.52, No.3, pp. 157-171 (2002).
15) Troncone, A.; "Numerical analysis of a landslide in soils with strain-softening behavior", Geotechnique, Vol.55, No.8, pp. 585-596 (2005).
16) Gerolymos, N.; "Numerical modeling of seismic triggering, evolution and deposition of rapid landslides: Application to Higashi-Takezawa (2004)", Int. J. Numer. Anal. Meth. Geomech., Vol.34, pp.383-407 (2010)
17) Yin, Y. P.; "Rapid and long run-out features of landslides triggered by the Wenchuan Earthquake", J. Eng. Geol., Vol.17, No.2, pp. 153-166 (2009), [in Chinese].
18) Sassa, K.; "Geotechnical model for the motion of landslides," Special Lecture of 5th International Symposium on Landslides, vol. 1, "Landslides", Balkema, Rotterdam, pp. 37-56 (1988).
19) Hungr, O.; "A model for the runout analysis of rapid flow slides, debris flows, and avalanches", J. Geotech. Eng., Vol.32, pp. 610-623 (1995).
20) Davies, T. R., McSaveney, M. J.; "Dynamic simulation of the motion of fragmenting rock avalanches", Can. Geotech. J., Vol.39, No.4, pp. 789-798 (2002).
21) Bhasin, R., Kaynia, M. A.; "Static and dynamic simulation of a 700-m high rock slope in western Norway", Eng. Geol., Vol.71, pp.213-226 (2004).
22) Wu, J. H., Lin, J. S., Chen, C. S.; "Dynamic discrete analysis of an earthquake-induced large-scale landslide", Int. J. Rock. Mech. Mining. Sci., Vol.46, No.2, pp. 397-407 (2008).
23) Tang, C. L., Hu, J. C., Lin, M. L., Angelier, J., Liu, C. Y., Chan, Y. C., Chu, H. T.; "The Tsaoling landslide triggered by the Chi-Chi earthquake, Taiwan: Insights from a discrete element simulation", Eng. Geol., Vol.106, pp. 1-19 (2009).
24) Cundall, P.A.; "A computer model for simulating progressive large scale movements in blocky rock systems", Proceedings of the Symposium of the International Society of Rock Mechanics, Nancy, France (1971).
25) Cundall, P.A.; "UDEC - A Generalized Distinct Element Program for Modeling Jointed Rock", Peter Cundall Associates, Report PCAR-1-80, U.S. Army, European research Office, London (1980).
26) Itasca Consulting Group, Inc.; UDEC–Universal distinct element code, Version 4.0 Manual, Itasca Consulting Group, Inc., Minneapolis (2004).
27) Chen, G. Q., Zheng, L. and Zen, K.; "A comparison between DDA and DEM in numerical simulations of earthquake induced landslides", Proc. of the International Symposium on Geomechanics and Geotechnics: From Micro to Macro, Shanghai, China (2010).